

Design of a multi-cusp ion source for proton therapy

WU Xiao-Bing(吴小兵)^{1,2} HUANG Tao(黄涛)¹ OUYANG Hua-Fu(欧阳华甫)¹

ZHANG Hua-Shun(张华顺)¹ GONG Ke-Yun(巩克云)¹

¹ Institute of High Energy Physics, CAS, Beijing 100049, China

² Graduate University of CAS, Beijing 100049, China

Abstract The permanent magnets of the discharge chamber in a multi-cusp proton source are studied and designed. The three electrode extraction system is adopted and simulated. A method to extract different amounts of current while keeping the beam emittance unchanged is proposed.

Key words multi-cusp proton source, discharge chamber, extraction system

PACS 29.20.Ej, 29.25.Nj

1 Introduction

Nowadays, proton therapy has become a very important method for cancer treatment after many years of clinical studies worldwide. The Advanced Proton Therapy Facility (APTF) is an accelerator-based project currently proposed in China. The accelerator complex consists of a 7 MeV linear accelerator as an injector and a 70–250 MeV slow cycling proton synchrotron. The linear accelerator consists of a 50 keV multi-cusp proton source driven by dual filaments, a Low Energy Beam Transport line (LEBT), a 2.5 MeV Radio Frequency Quadrupole (RFQ) accelerator and a 7 MeV Drift Tube Linear (DTL) accelerator. The proton therapy facility has rigorous requirements of the ion source and LEBT for their reliability, repetition, life time and maneuverability. At present, there are many kinds of ion source that can meet the requirements, such as cold cathode ion sources [1], RF ion sources [2] and hot cathode ion sources [3]. Both the cold cathode and RF ion source need the initial electron. Sometimes it is hard to initiate the arc pulse, so the hot cathode ion source becomes a good candidate. There are many types of hot cathode ion source, such as multi-cusp ion sources [4, 5], duo-plasma ion sources, Penning ion sources and crossed field ion sources. Both the multi-cusp and duo-plasma ion sources have good performance in pulse repetition, symmetric beam, low extraction beam emittance and technology maturity. In particular, the former is of simpler structure and offer easier operation. As a result, the multi-cusp ion source

driven by dual filaments is adopted as the APTF ion source. In Table 1, some design parameters of the ion source are listed.

Table 1. APTF multi-cusp ion source design parameters.

| ion type | proton |
|--|--------|
| pulse current/mA | 10 |
| proton ratio(%) | > 70 |
| extraction energy/keV | 50 |
| emittance/($\pi\text{mm}\cdot\text{mrad}$ norm.rms) | < 0.15 |
| pulse width/ μs | 36.25 |
| repetition rate/Hz | 0.5 |
| life time/h | > 1000 |

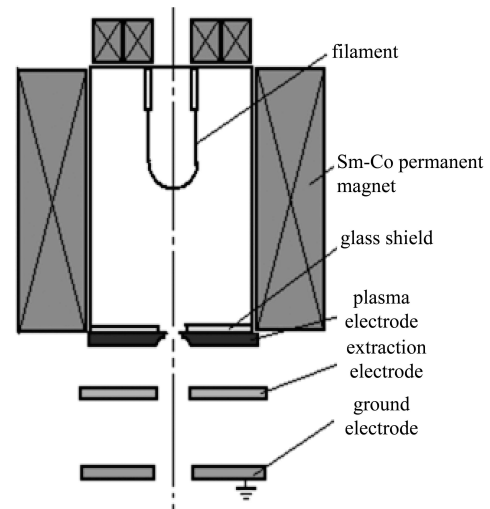


Fig. 1. Scheme of a multi-cusp proton source discharge chamber and extraction system.

Received 29 January 2010

©2010 Chinese Physical Society and the Institute of High Energy Physics of the Chinese Academy of Sciences and the Institute of Modern Physics of the Chinese Academy of Sciences and IOP Publishing Ltd

The scheme of a multi-cusp proton source discharge chamber and extraction system is shown in Fig. 1. The chamber mainly consists of a stainless steel source body, two filaments, several Sm-Co permanent magnets and a glass shield that is used to enhance the plasma density and proton content. The size of the permanent magnet is $17\text{ mm} \times 12\text{ mm} \times 100\text{ mm}$ and the surface magnetic field is larger than 0.35 T [6]. The extraction system contains a plasma electrode, an extraction and a ground electrode.

2 Multi-cusp ion source discharge chamber

To obtain a dense, stable and uniform plasma, a certain magnetic field free region ($B < 20\text{ G}$) is required [7]. It is obvious that the field free region increases with the inner diameter of the chamber. However, with increasing chamber diameter, it will cause other problems. So to ensure the optimal inner diameter of the chamber, the following modeling is carried out.

2.1 Two dimensional modeling

The 2-dimensional code Poisson has been used for the modeling. In order to obtain a wide centric region with a field free enough for installing the dual filaments, different numbers of the magnet and inner radius of the chamber have been calculated during modeling. The results are shown in Fig. 2.

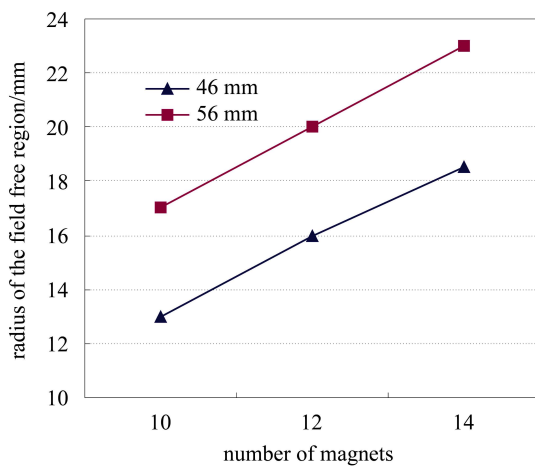


Fig. 2. Variation of the radius of the field free region with the number of magnets at different inner radii of the chamber.

As seen from Fig. 2, the radius of the centric field free region is increased with the number of magnets and the inner radius of the discharge chamber. Compared with the inner radius of the chamber, the effect of the magnet number on the radius of the field free region is more remarkable. Finally, 12 permanent magnets and an inner radius of 50 mm are chosen for the ion source. The magnetic field distribution in the chamber is shown in Fig. 3.

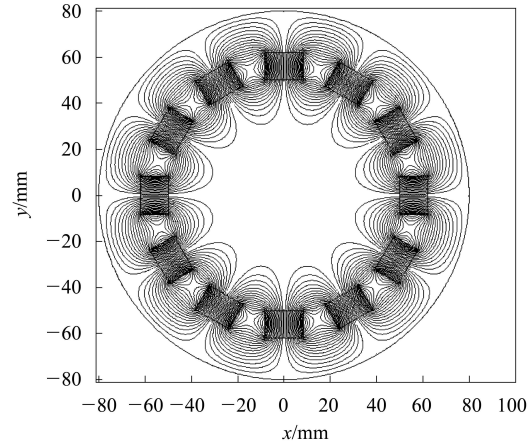


Fig. 3. The magnetic field distribution in the discharge chamber.

Obviously, the magnetic field is axially symmetric. The distribution diagram of the magnetic field intensity on the x axis is shown in Fig. 4.

As seen in Fig. 3 and Fig. 4, the centric field free region ($B < 20\text{ G}$) in the discharge chamber is almost a circle with a radius of about 17.5 mm . The magnetic field is about 2500 G at the discharge chamber wall. This is enough to confine the plasma to the discharge chamber [8].

2.2 Three dimensional modeling

A 3-dimensional code has been used for the modeling. As shown in Fig. 5, 14 Sm-Co permanent magnets are adopted in the simulation.

There are 12 permanent magnets around the discharge chamber and 2 magnets on top of the discharge chamber. The size of permanent magnet is $17\text{ mm} \times 12\text{ mm} \times 100\text{ mm}$ and the surface remnant magnetic field $B_r = 1.1\text{ T}$. They all act as confinement magnets to confine the plasma. The structure of the discharge chamber is also shown in the figure. The chamber is made of stainless steel with an inner radius of 50 mm and a thickness of 3 mm . The distribution of the magnet field intensity along the x axis is shown in Fig. 6.

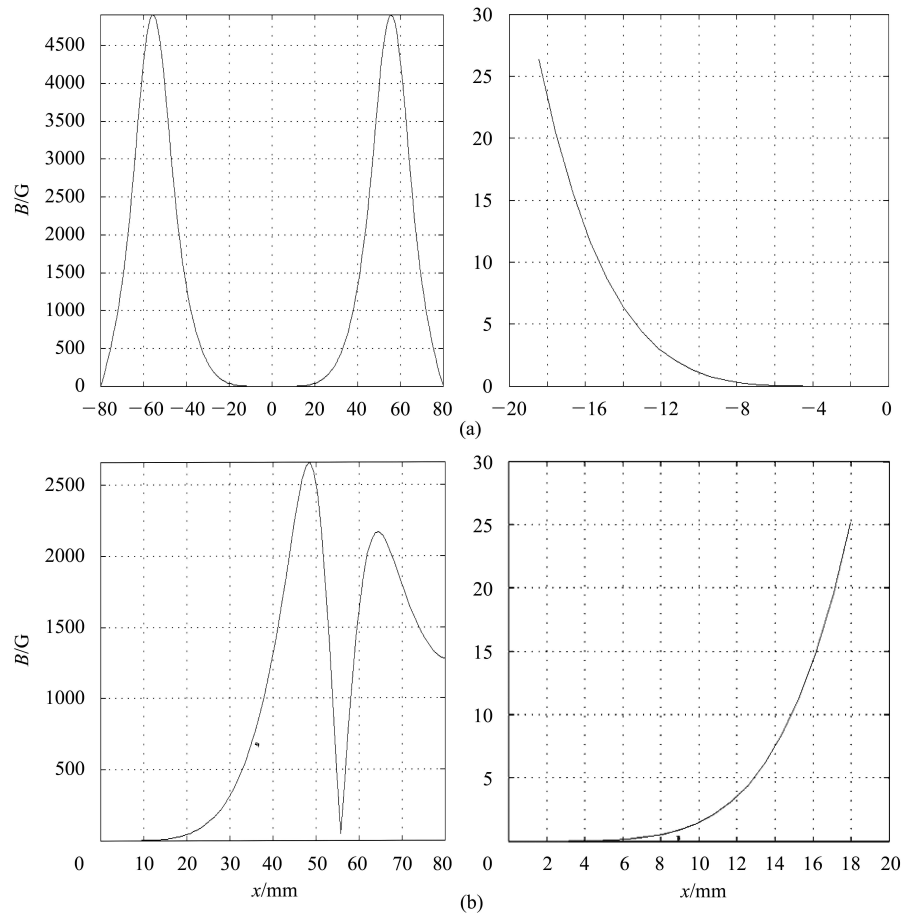


Fig. 4. (a) Magnetic field intensity distribution along the center of the magnet; (b) magnetic field intensity distribution along the center of the two magnets.

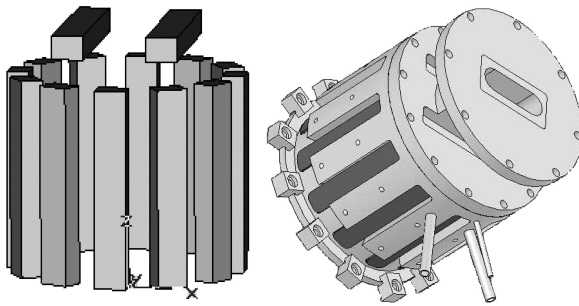


Fig. 5. Distribution of the magnets and the structure of the discharge chamber.

As seen in Fig. 6, the centric field free region is almost a circle with a radius of about 16.5 mm. The result here is basically consistent with the two dimensional modeling result. Due to the fringe field of the magnet end, the radius is a little smaller than that of the former. Because there are two top permanent magnets, the B field intensity distribution along the z axis must also be taken into account. The result is shown in Fig. 7.

As seen in Fig. 7, the depth of the field free region in the discharge chamber is about 21.57 mm.

In conclusion, the field free region in the discharge chamber is a cylinder of 16.5 mm in radius and 21.57 mm in depth, and the cylinder is near the extraction aperture. The contour graph is shown in Fig. 8.

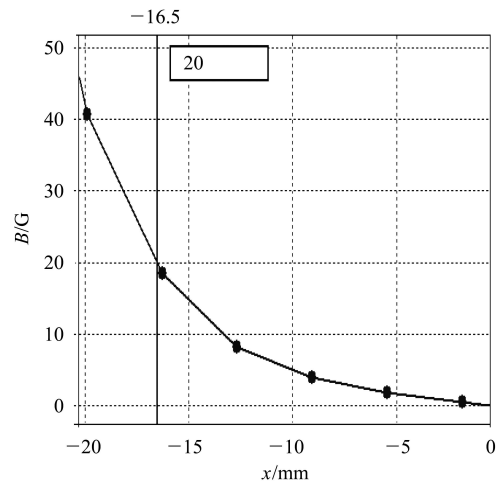


Fig. 6. Magnetic field intensity distribution along the x axis.

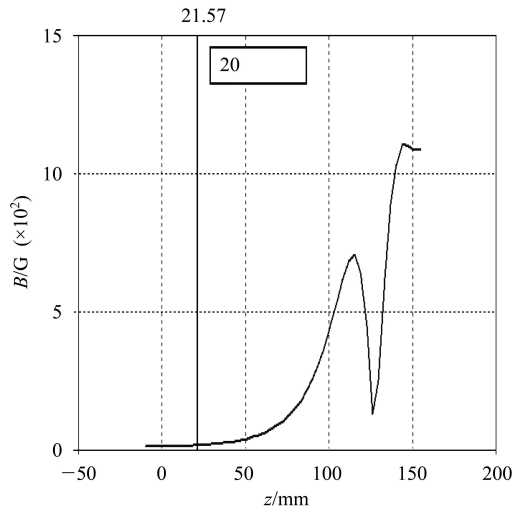


Fig. 7. Magnetic field intensity distribution along the z axis.

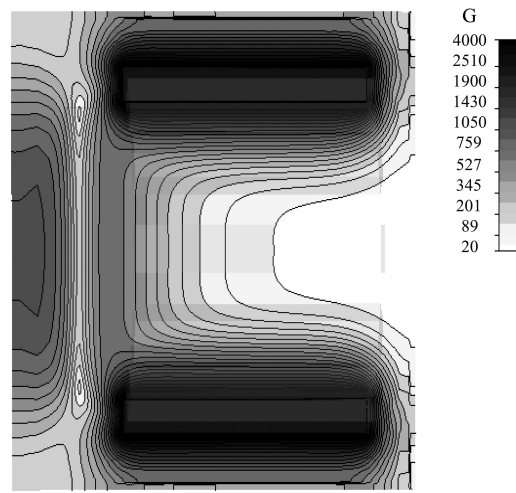


Fig. 8. B contour graph at $x = 0$ plan.

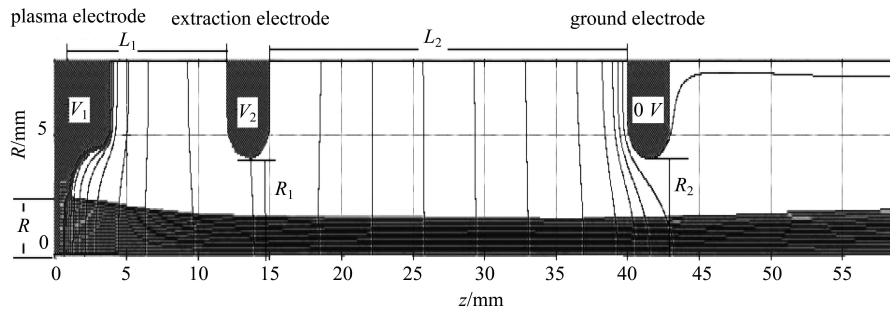


Fig. 9. The structure of the extraction system.

3 Extraction electrodes

The structure of the extraction system consists of a plasma electrode, an extraction electrode and a ground electrode [9, 10]. The code PBGUN has been used for beam optical modeling. The structure of the extraction system and the beam trajectory are shown in Fig. 9.

To extract the 10 mA, 50 keV proton beam, the optimal parameters are confirmed during modeling. The potential of the plasma electrode V_1 and extraction electrode V_2 are equal to 50 kV and 15 kV, respectively. The distance between the plasma and the extraction electrode L_1 is equal to 11 mm. The distance between the extraction and ground electrode L_2 is equal to 25 mm. The radius of the plasma electrode aperture R_1 and the extraction (ground) electrode R_2 is 2.5 mm and 4 mm, respectively. When the optimal parameter is satisfied, the extraction beam has the lowest emittance at the measure point. The emittance plot is shown in Fig. 10.

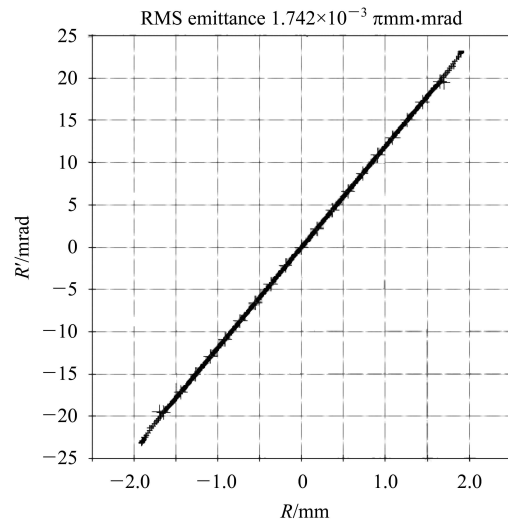


Fig. 10. The optimal beam emittance at the measure point.

During proton therapy, the beam current should be changed when “four dimensional beam scanning” (beam current and three coordinates of the beam scanning spot) technology is used. It is better to extract different beam currents from the ion source

while keeping the beam emittance unchanged. To obtain a beam with invariable optimal emittance at different beam currents, the voltage of the extraction electrode should change with the increasing of the beam current. The result is shown in Fig. 11.

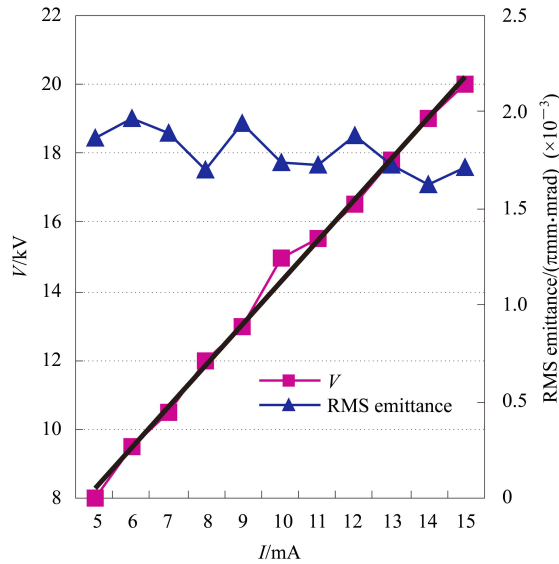


Fig. 11. Voltage of the extraction electrode (square) and RMS emittance (triangle) versus the beam current.

As seen in Fig. 11, the voltage of the extraction electrode varies almost linearly with increasing beam current, while the RMS emittance stays basically unchanged along the optimal emittance. All of the RMS emittances are smaller than $2.00\text{E-}03 \pi\text{mm}\cdot\text{mrad}$, which is much lower than the designed RMS acceptance ($0.15 \pi\text{mm}\cdot\text{mrad}$) of the RFQ. The ratio of the Twiss parameter α and β versus the beam current is shown in Fig. 12.

As shown in Fig. 12, $-\alpha/\beta$ increases with the beam current when the beam current is smaller than 8 mA, while the value of $-\alpha/\beta$ varies very slowly.

As we know, the ratio $-\alpha/\beta$ stands for the direction of the phase ellipse. Therefore, when the beam current varies in the region of the designed beam current value of 10 mA, the parameters of the solenoid magnets in the LEBT do not need any adjustment to match the RFQ for the designed acceptance ($0.15 \pi\text{mm}\cdot\text{mrad}$) of the RFQ is much larger than the emittance $2.00\text{E-}03 \pi\text{mm}\cdot\text{mrad}$. Even if the beam current is smaller than 8 mA, the beam can be matched into the RFQ by slightly adjusting the parameters of the solenoid magnets in the LEBT. This way of changing the beam current is useful in the actual operation, because the entire downstream accelerator parameters keep constant.

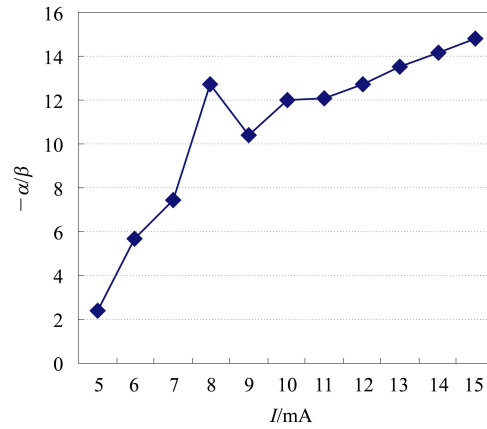


Fig. 12. $-\alpha/\beta$ versus the beam current.

4 Conclusions

The discharge chamber and the extraction system of the multi-cusp proton source are confirmed during the analysis. The discharge chamber uses 12 permanent magnets with the inner radius equal to 50 mm. A method to extract different currents while keeping the beam emittance unchanged is proposed.

References

- 1 Bugrova G E, Kondranina S K, Kralkina E A et al. *Current Applied Physics*, 2003, **3**: 485–489
- 2 Spadtke P, Bossler J, Emig H et al. *Nuclear Instrument and Methods in Physics Research B*, 1998, **139**: 145–149
- 3 Joshi N, Droba M, Meusel O et al. *Nuclear Instrument and Methods in Physics Research A*, 2009, **606**: 310–313
- 4 Lee Y, Gough R A, Kunkel W B et al. *Nuclear Instrument and Methods in Physics Research B*, 1996, **119**: 543–548
- 5 Lee Y, Perkins L T, Gough R A et al. *Nuclear Instrument and Methods in Physics Research A*, 1996, **374**: 1–4
- 6 Huck H, Digregorio D E, Fernandez J O et al. *Nuclear Instrument and Methods in Physics Research B*, 2001, **175**: 772–776
- 7 ZHANG Hua-Shun. *Ion Sources*. Beijing: Science Press, 1999. 204
- 8 Wutte D, Freedman S, Gough R et al. *Nuclear Instrument and Methods in Physics Research B*, 1998, **142**: 409–416
- 9 Reijonen J, Heikkinen P, Liukkonen E et al. *Review of Scientific Instruments*, 1998, **69**(2): 1138–1140
- 10 JIA Xian-Lu, ZHANG Tian-Jue, LU Yin-Long et al. *Chinese Physics C (HEP&NP)*, 2008, **32**(Supp. I): 265–267